

DOI: 10.3727/096368911X580518

CT-0318 Accepted 3/05/2011 for publication in "Cell Transplantation"

Human adipose tissue as a source of cells with angiogenic potential

Krisztina Szöke, Karen Johanne Beckstrøm, and Jan E. Brinchmann

Norwegian Center for Stem Cell Research, Institute of Immunology, Oslo University Hospital, Rikshospitalet and Institute of Basic Medical Sciences, University of Oslo
PO Box 1121 Blindern, 0317 Oslo, Norway

Running head: Adipose tissue derived endothelial cells

Corresponding author: Jan E. Brinchmann

Mailing address: Norwegian Center for Stem Cell Research, Institute of Immunology, Oslo University Hospital, Rikshospitalet and Institute of Basic Medical Sciences, University of Oslo, PO Box 1121 Blindern, 0317 Oslo, Norway

E-mail address: Jan.Brinchmann@rr-research.no

Phone: +47 22 84 04 89

Fax: +47 22 85 10 58

ABSTRACT

Endothelial cells (EC) are involved in the process of angiogenesis, the outgrowth of new vessels from pre-existing blood vessels. If available in sufficiently large numbers, EC could be used therapeutically to establish blood flow through in vitro engineered tissues and tissues suffering from severe ischemia. Adipose tissue (AT) is an easily available source of large number of autologous EC. Here we describe the isolation, in vitro expansion and characterization of human AT derived EC (AT-EC). AT-EC proliferated rapidly through 15 – 20 population doublings. The cultured cells showed cobblestone morphology and expressed EC markers including CD31, CD144, eNOS, CD309, CD105, von Willebrand factor, CD146, CD54 and CD102. They bound *Ulex europaeus* agglutinin I lectin and took up DiI-Ac-LDL. The AT-EC formed capillary-like tubes in Matrigel in vitro and formed functional blood vessels in Matrigel following subcutaneous injection into immunodeficient mice. In conclusion, AT-EC reach clinically significant cell numbers after few population doublings and are easily accessible from autologous AT, which also contains mesenchymal stem cells/pericytes. Thus AT yields two cell populations which may be used together in the treatment of tissue ischemia and in clinical applications of tissue engineering.

Key words: adipose tissue; endothelial cells; vasculogenesis; tissue ischemia; tissue engineering

INTRODUCTION

Therapeutic strategies based on the delivery of angiogenic cells have been attempted for peripherovascular disease (40,46) and ischemic heart disease (9), so far with modest functional improvement. Generation of new blood vessels is also a major issue in tissue engineering (20,32,39). Here different approaches have been used to overcome the problem of vascularization, such as incorporation of angiogenic factors into the engineered tissues to promote the ingrowth of microvessels, prevascularization of matrices prior to cell seeding and seeding of endothelial cells (EC) along with other cell types (27). However, to date no cell-based therapeutic strategy has been able to robustly generate new blood vessels in engineered or ischemic tissues.

The most popular candidates for strategies of cell-based therapeutic neovascularization are the endothelial progenitor cells (EPC) (14,32). EPC were first isolated from human peripheral blood by Asahara et al (2). Two distinct EPC populations are observed with different growth characteristics, which are referred to early- and late-outgrowth EPC (31). Recently, the vasculogenic potential of EPC from adult peripheral blood and human cord blood were described and compared (24). EPC from cord blood were found to be superior to adult cells both in proliferative potential and vasculogenesis, but the vasculogenic capacity of both populations deteriorated rapidly with time in cell culture. In another study, endothelial colony-forming cells were isolated from unmanipulated human peripheral blood (34). These cells are easily available, but because the precursor frequency is low, prolonged in vitro cell expansion will be required in order to get an appropriate number of cells for therapy.

Mature EC can also be candidates for cell therapy applications. These cells are mostly derived from the umbilical vein or the aortic endothelium. Both these populations may

be expanded in vitro, although they do not normally proliferate over many passages (17). However, in terms of human cell therapy, the main problem associated with the use of these cells is that they will always be allogeneic to the patient, and therefore likely to be rejected by immunological mechanisms. Microvascular EC (MVEC) resemble late-outgrowth EPC (3). As such, they should be promising cells for therapeutic neovascularization. However, MVEC are most commonly obtained from sources such as newborn foreskin, the retina and the myometrium, all sources that in practical terms will be allogeneic to the patient.

Adipose tissue (AT) is an easily available source of large number of autologous cells for cell therapy applications. Mesenchymal stem cells (MSC) from AT have been isolated and characterized (4,49), and are currently being tested in clinical trials (12). MSC are frequently obtained from the stromal-vascular fraction (SVF) of AT cells. The SVF of AT cells has also been shown to contain cells with angiogenic potential (30,33). Several attempts have been made to isolate EC from SVF using differential plastic attachment and positive selection strategies (1,10,18,19,37). However, there is still a need for data on the phenotype of the AT-EC population, and how the phenotype and gene expression of this cell population is modulated by in vitro culture. This sort of data, combined with experiments showing that the cells are able to form vessels in vivo, are required before AT-EC may be accepted for clinical trials of EC transplantation.

Here we describe the isolation, purification, expansion and extensive characterization, both at the uncultured and cultured stage, of the EC population obtained from the SVF from AT. Based on our previous observation that most of the AT-EC did not express CD44, while the majority of AT-MSC did express this marker (4), we chose to purify the AT-EC from the SVF by removing CD44⁺ cells. We demonstrate that AT-EC have

endothelial morphology and phenotype, that they form capillary-like tubes in Matrigel in vitro and functional blood vessels in vivo. One important aspect of these cells, which separate them from other EC, is that they derive from a source which is easily accessible in all patients. They can be obtained in very large numbers, which means that clinically relevant numbers of cells can be obtained after only a few population doublings in vitro. Importantly, they derive from a tissue which also yields MSC (4,49,50). Recent studies on MSC populations suggest that these derive from blood vessel walls and that they may in fact be identical to the pericytes (5-7). Small blood vessels are composed of EC surrounded by basal lamina and loosely covered by pericytes, which are embedded in the basement membrane of the microvessels underlying the EC (23,38,41). The pericytes play a role in vascular stabilization by interaction with EC (42) and can stimulate angiogenesis (26,45). Thus, AT may provide two cell populations required for vasculogenesis.

CELL TRANSPLANTATION
The Regenerative Medicine Journal

MATERIALS AND METHODS

All reagents were purchased from Sigma Aldrich, St. Louis, MO unless otherwise stated.

Isolation of AT-EC

AT was obtained from liposuction material from abdominal regions of three healthy female donors (age 24–40) undergoing cosmetic surgery. The donors provided informed consent, and the collection and storage of AT, AT-EC and AT-MSC were approved by the regional committee for ethics in medical research. The SVF was separated from AT as described previously (4). Briefly, lipoaspirate (300–600 ml) was washed repeatedly

to remove erythrocytes and leukocytes with Hanks' balanced salt solution (HBSS; Gibco, Invitrogen, Paisley, UK) containing antibiotics (100 IU/ml penicillin and 100 IU/ml streptomycin) and 2.5 µg/ml amphotericin B. This material was then digested for 75 min using 0.1% collagenase A type 1 at 37°C applying constant gentle rotation. Following centrifugation at 400 x g for 10 min at room temperature the pellet was re-suspended in HBSS containing antibiotics and 2% fetal bovine serum (FBS; BioWhittaker, Lonza, Verviers, Belgium), and the cells were filtered through 100 µm and then 40 µm cell sieves (Becton Dickinson, San Jose, CA). SVF cells were obtained from the interface after Lymphoprep gradient separation (Axis Shield, Oslo, Norway) at 400 x g for 30 minutes, washed and re-suspended in HBSS containing antibiotics and 2% FBS. Cell counts and viability assessment were performed using acridine orange/ethidium bromide staining and a fluorescence microscope (Eclipse E600, Nikon, Kanagawa, Japan). To obtain AT-EC from the SVF, CD44⁺ cells were removed using Dynabeads (Dynabeads Pan Mouse IgG, Invitrogen Dynal AS, Oslo, Norway) according to the manufacturer's description. Briefly, Dynabeads were washed, then pre-coated with monoclonal anti-CD44 antibody (Caltag Laboratories, Invitrogen, Carlsbad, CA) at the concentration of 0.6µg antibody per 25µl Dynabeads and incubated for 2 hours with gentle tilting and rotation. Dynabeads were then washed again and approximately 400x10⁶ magnetic CD44 beads were added to 100x10⁶ SVF.

In vitro expansion of AT-EC

AT-EC were plated at 2 x 10⁶ cells per 75-cm² tissue culture flask (Nunc, Roskilde, Denmark) coated with 1% gelatin. Cells were maintained at 37 °C in an atmosphere of

5% CO₂ in humid air using EC growth medium (MCDB 131; Gibco) supplemented with 7.5% FBS, 1% L-glutamine, 1ng/ml basic fibroblast growth factor, 1μg/ml hydrocortisone, 10ng/ml epidermal growth factor, 50μg/ml Gentamicin and 250ng/ml Amphotericin B. Cells still in suspension were removed on day 4-5 and the medium was replaced. When the cells reached 80-90% confluency, cell adherence was interrupted by trypsin-ethylenediaminetetraacetic acid (EDTA) solution for EC and the cells were inoculated into new flasks at 10,000 cells per cm². Additional purging of contaminating cells was performed using anti-CD44 coated Dynabeads if required at the first passage. Cells were routinely passaged every 3-4 days. Viable cells were counted at each passage. Growth curves were generated using GraphPad Prism version 5 software (GraphPad Software Inc., La Jolla, CA).

Isolation and in vitro expansion of AT-MSC

To obtain AT-MSC/pericytes for the Matrigel vascularization studies the CD44⁺ cells positively selected from the SVF of the same donors were cultured in Dulbecco's modified Eagle's medium/F12 (Gibco) containing 10% FBS and antibiotics. To remove remaining CD45⁺ leukocytes, at p2, magnetic beads directly coupled to mouse anti-human CD45 monoclonal antibodies (Caltag Laboratories), as described above, were mixed with the CD44 depleted cells at a ratio of 4 beads per cell. After 2 hours of incubation the CD45⁺ cells attached to beads were removed using a magnet, and the remaining cells were placed back in cell culture for further in vitro expansion.

Characterization of AT-EC

The isolated AT-EC from all the three donors were characterized at the uncultured stage (p0), at early (p2), middle (p6) and late (p12) passages. The endothelial nature of the cells was confirmed by real-time reverse transcription-polymerase chain reaction (RT-

PCR), flow cytometry, *Ulex europaeus* agglutinin I lectin (UEA-1) binding and DiI complex acetylated low-density lipoprotein (DiI-Ac-LDL) uptake as well as in vitro and in vivo angiogenesis assays.

Real-time RT-PCR analysis

Total RNA was extracted from cells at different passages using RNAqueous - Micro Kit (Applied Biosystems/Ambion, Austin, TX) according to the manufacturer's protocol and treated with DNase I (Applied Biosystems/Ambion). Reverse transcription (RT) was performed using High-Capacity cDNA Reverse Transcription Kit (Applied Biosystems, Foster City, CA) following the manufacturer's protocol with 200 ng total RNA per 20 μ l RT reaction. Relative quantification was performed using the 7300 Real-time RT-PCR system (Applied Biosystems) and TaqMan Gene Expression Assay (Applied Biosystems) reagents according to the manufacturer's description. The thermocycler parameters were 95°C for 10 min followed by 40 cycles of 95°C for 15 sec and 60°C for 1 min. All primers are provided in Table 1. All samples were run in triplicates. After verifying the stable expression of *CDKN1A*, this gene was selected as endogenous control. The mRNA levels were normalized to the expression of *CDKN1A* for each sample. Relative mRNA levels were calculated by the comparative CT method, where the threshold cycle (CT) values are given by the $2^{-\Delta\Delta Ct}$ formula (22). Differential expression of all markers was calculated in relation to the corresponding uncultured cells. Graphs were created with GraphPad Prism version 5 software. As a positive control, primary adult human dermal MVEC (p6) were purchased from PromoCell GmbH (Heidelberg, Germany). Human AT-MSC and chondrocytes were used as negative controls for the endothelial phenotype.

Flow cytometry

Flow cytometry was performed for determination of cell surface antigen expression of freshly isolated (uncultured) and cultured (p2, p6 and p12) AT-EC from three different donors and of human dermal MVEC (p6). All monoclonal antibodies are provided in Table 2. Irrelevant control antibodies were included for each of the different fluorochromes. Cells were incubated with directly conjugated antibodies for 10 min, washed with phosphate-buffered saline (PBS) containing 1% FBS and fixed in 1% paraformaldehyde (PFA). Cells were analysed using a FACSCalibur flow cytometer applying BD CellQuest Pro Software (BD Biosciences).

Intracellular staining for von Willebrand factor

Flow cytometry was performed for determination of intracellular expression of von Willebrand factor (vWF) in freshly isolated (uncultured) and cultured (p2, p6 and p12) AT-EC from three different donors. For intracellular staining, a BD Cytofix/Cytoperm Fixation/Permeabilization kit (BD Biosciences) was used according to the manufacturer's description. Briefly, cells were trypsinized, washed, centrifuged then re-suspended in BD Cytofix/Cytoperm buffer. After 20 min incubation cells were washed in 1x BD Perm/Wash buffer, incubated for 30 min on ice with mouse anti-human vWF (Immunotech, Marseille, France). Cells were washed once again, incubated for 30 min on ice with goat anti-mouse Ig (H+L)-R-Phycoerythrin (RPE) (Southern Biotech), washed and finally fixed with 1% PFA and analyzed by a FACSCalibur flow cytometer applying BD CellQuest Pro Software. As a negative control secondary antibody alone was used to assess nonspecific fluorescence.

DiI-Ac-LDL uptake

To assess the uptake of DiI-Ac-LDL (Molecular Probes, Invitrogen, Eugene, OR), AT-EC and AT-MSC were seeded on gelatin-coated chamber slides (BD Falcon 4.0 cm²/chamber, BD Biosciences). After reaching confluence, cells were washed once with medium then incubated in medium containing 15µg/ml of DiI-Ac-LDL for four hours in a culture incubator at 37°C with 5% CO₂. Then the cultures were washed with PBS and cells were fixed in 4% PFA. After fixation cells were washed again. Human chondrocytes were used as a negative control. All immunocytochemistry and immunohistochemistry slides were mounted with Vectashield mounting medium for fluorescence containing 4',6-diamidino-2-phenylindole (DAPI) (Vector Laboratories Inc., Burlingame, CA) for nuclear visualization. The incorporation of DiI-Ac-LDL was visualized using a Nikon Eclipse E600 fluorescent microscope (Nikon, Kanagawa, Japan) equipped with Leica DC 300F (Leica Microsystems DI, Cambridge, UK) and Color View III (Olympus, <http://www.olympus-global.com/en/>) digital cameras. Pictures were taken by Adobe Photoshop 7.0 (Adobe Systems Norge AS, Oslo, Norway) and Cell-B software (Olympus).

In vitro tube forming assay

Matrigel Basement Membrane Matrix (BD Biosciences) was used as a substrate for vasculogenesis assays to determine the functional ability of the isolated cells to form networks. 50µl of Matrigel was spread at the bottom of 96 well plates (Costar, Corning, New York, NY) and used as a coat upon which freshly isolated (uncultured) and cultured (p2, p6 and p12) AT-EC were seeded in 100µl medium. Human dermal MVEC (p6) were used as a positive control. AT-MSC alone and mixed with AT-EC were also

tested in this assay. Cultures were incubated at 37°C in a humidified incubator with 5% CO₂ for 16-20 hours. The presence of tubes was visualized using a Leica DMIL inverse microscope (Leica Microsystems, Wetzlar, Germany). The assay was performed in triplicates. PKH67 Fluorescent Cell Linker Kit was used to label the cells for the fluorescence image. Images were taken with a Leica DFC 320 camera (Leica Microsystems Wetzlar, Germany) using Adobe Photoshop 7.0 software.

In vivo vasculogenesis assay

AT-EC from donor 2 at 0.3×10^6 , 0.5×10^6 and 2×10^6 , alone or combined with AT-MSC from the same donor (4:1 ratio) were re-suspended in 50 μ l PBS, mixed with 200 μ l of Matrigel on ice and injected subcutaneously into 8 weeks old nonobese diabetes/severe combined immunodeficiency (NOD/SCID) mice. Each experimental condition was performed with 2 mice. Animal experiments were approved by the National Animal Research Authority.

The Matrigel plugs were removed after 6 weeks, fixed in 10% PFA (Electron Microscopy Sciences, Hatfield, PA) overnight, embedded in paraffin and sectioned. For evaluation of the angiogenic potential, 3 μ m thick sections were stained for morphological evaluation using hematoxylin and eosin (data not shown). For immunohistochemistry analysis sections were deparaffinized, then boiled in PBS containing 0.05% citraconic anhydride (pH 7.4) for 20 minutes for epitope retrieval. Mouse anti-human CD31 primary antibody at 1:20 (DAKO) was applied overnight in a humidified chamber at 4°C diluted in PBS containing 1.25% bovine serum albumin (BSA) and 0.1% saponin (SERVA Electrophoresis GmbH, Heidelberg, Germany) for blocking and permeabilization. Slides were washed three times in PBS. Human vessels

were detected using cyanine 3 (CY3)-conjugated donkey anti-mouse IgG (1:600; Jackson ImmunoResearch) at room temperature for 1.5 hours. Unbound antibody was removed with three washes in PBS. Double staining with fluorescein isothiocyanate (FITC) conjugated UEA-1 at 1:200 was performed together with the secondary antibody incubation step. As a control, secondary antibody alone was used to assess nonspecific fluorescence.

Data analysis

Data are shown as mean \pm SEM and determined using GraphPad Prism version 5 software.

RESULTS

Morphology and in vitro growth characteristics of AT-EC

Because AT-EC are abundant within the SVF, even after purging of non-endothelial cells we could obtain $15\text{--}60 \times 10^6$ cells from 300–600 ml liposuction material, of which $8\text{--}10 \times 10^6$ were seeded for further analysis. Cell yield was $67.2 \times 10^3 \pm 20.3 \times 10^3$ (mean \pm SEM) cells per ml of lipoaspirate.

AT-EC colonies emerged after 4-5 days in the culture. The cultures exhibited the classical EC cobblestone morphology from p1 and maintained their morphological characteristics for as long as cell proliferation continued (Figure 1A). AT-EC quickly entered a phase of logarithmic growth (Figure 1B). During this phase, the population doubling time was 2.3 days. The proportion of AT-EC that were able to attach and form colonies was difficult to quantify. However, when the cells were passaged for the first time, after 8 days, the cell number was unchanged (2 donors) and doubled (1 donor). Considering the population doubling time, this suggests that approximately half of the

cells attached and formed colonies. Logarithmic growth ceased for cells from two donors at p14, and for one donor at p19.

Gene expression in AT-EC

The endothelial nature of these cells was examined in a number of different ways. Figure 2 shows the expression of genes relevant to the endothelial lineage and to the mesenchymal lineage, as AT-MSC were also present in SVF and could be contaminating the AT-EC. The expression of these genes was calculated relative to the expression of the endogenous control gene *CDKN1A*. Relative to the expression in uncultured AT-EC, the mRNA levels for platelet endothelial cell adhesion molecule-1 (*PECAM1*), Vascular endothelial cadherin (*CDH5*), Vascular endothelial growth factor receptor 2 (*KDR*) and von Willebrand factor (*VWF*) were uniformly up-regulated in cultured cells at p2, and then remained stably expressed. *CD34*, *CD90* (*THY1*) and endothelial nitric oxide synthase (*NOS3*) showed some between-donor variation, but the trend was for an over-all relatively stable expression of these genes. The mRNA expression levels of the endothelial lineage genes in the cultured AT-EC were similar to the commercially available human MVEC whereas the expression levels of *THY1* and *CD44* were higher in the AT-EC (Figure 3). In human chondrocytes, which were used as a negative control, endothelial markers *PECAM1*, *CD34*, *NOS3*, *CDH5*, *KDR* and *VWF* were not expressed. However, *CD44* and *THY1* were expressed at high levels (data not shown).

Flow cytometry analysis

To examine the efficiency of our isolation technique and possible phenotypic changes due to in vitro expansion, flow cytometry analysis was performed. Figure 4A shows the distribution of the $CD31^+$, $CD44^+$, $CD45^+$ and $CD90^+$ cell populations in the SVF.

Figure 4B shows that after the removal of CD44⁺ cells from the SVF, 4% of CD44⁺ cells remained in the cell suspension. Of the CD44⁻ cells, 80% were CD31⁺, and 87% were CD90⁺. However, despite the low proportion of CD44⁺ cells present after the initial isolation, some of the cultured cells appeared as fibroblastoid toward the first passage. Therefore, to minimize the contamination by non-endothelial cells, we repeated the removal of CD44⁺ cells at the first passage. This resulted in a >95% CD31⁺ endothelial cell culture with <2% CD44⁺ cells contaminating the AT-EC culture at p2. In the course of cell culture, an increasing proportion of the AT-EC expressed CD44, so that for this donor, 77% of the cells were CD44⁺ at p12, despite retaining cobblestone morphology and being almost uniformly CD31⁺. This observation was made for cells from all the donors, and substantiated the increasing expression of *CD44* mRNA shown in Figure 2.

Of the uncultured CD31⁺ cells, 90% were also strongly CD90⁺. However, the surface expression of CD90 was quickly lost, so that at p2 hardly any surface expression of CD90 was observed for any of the donors (Figure 4B). Interestingly this was not a reflection of the mRNA expression for *THY1*, which was maintained practically unchanged through p6, and also through p12 for two of the donors (Figure 2). A similar observation was made for CD34, which was expressed on the surface of most of the uncultured cells, but then quickly and persistently disappeared from the surface (Figure 5A). At the mRNA level, expression was maintained for two of the donors, and reduced at p6 and p12 for the last donor.

Figure 5 shows that uncultured AT-EC express endothelial markers such as CD34, CD144, CD146, CD105, human lymphocyte antigen (HLA) DR, CD54, CD102, vWF and UEA-1. The expression of most of these molecules was high and persistent in the

cultured cells. However, for HLA DR the expression disappeared at p2, and for CD144 there was a tendency to reduced expression in cultured cells. Interestingly this observation, too, was in contrast to the changes observed for CD144 (*CDH5*) at the mRNA level, where expression was higher in the cultured cells (Figure 2). AT-EC were uniformly negative for CD133/1 and CD133/2, which have been used as markers for EPC (3). They expressed moderate levels of VEGFR-1 and VEGFR-2 at the uncultured state. The expression of VEGFR-1 was reduced or absent in the cultured cells, while VEGFR-2 was upregulated both at the protein and the mRNA level in these cells. The cells were negative at all times for the hematopoietic surface antigens CD45, CD14, CD19 and CD3 (data not shown).

Human dermal MVEC were used as a positive control for the examination of the endothelial and mesenchymal cell surface antigen expression (Figure 3C). As expected there were some differences in the surface marker expression between the two cell populations. The MVEC did not express CD44 during the culture, whereas CD34 was expressed on the surface of a proportion of the cells.

DiI-Ac-LDL uptake

Figure 6 shows that AT-EC take up DiI-Ac-LDL (Figure 6A). This characteristic is common for EC and further indicates the endothelial properties of the cultured cells. Human chondrocytes and AT-MSC did not take up DiI-Ac-LDL (Figure 6B and C, respectively).

In vitro and in vivo vasculogenesis assays

The freshly isolated cells did not form vascular tubes when seeded on Matrigel (Figure 7A), while the cultured cells both at early (Figure 7B and C) and late passage (Figure 7D) formed capillary-like structures, similar to the commercially obtained MVEC

(Figure 3B). AT-MSC alone (Figure 7E) or AT-MSC mixed with AT-EC (Figure 7F) formed single tube-like structures, but not the extensive vascular network formed by the AT-EC alone.

To determine if AT-EC could form functional blood vessels *in vivo*, 0.3×10^6 , 0.5×10^6 and 2×10^6 of AT-EC were mixed with Matrigel and implanted into NOD/SCID mice. In addition, because MSC have been shown to be identical to pericytes *in vivo* and thus might improve the vasculogenic properties of the AT-EC, AT-MSC from the same donor were mixed into the Matrigel in half of these experiments. The implants were removed and evaluated at six weeks. Where AT-EC were applied at 0.5×10^6 and 2×10^6 per Matrigel, either alone or combined with AT-MSC, tubular vessel-like structures could be identified (Figure 8). The degree of vascular network formation tended to be greater when combined cell populations were applied. The vessels were human-derived, as they stained with antibodies specifically recognizing human CD31 and UEA-1 (Figure 8A-F). The presence of mouse red blood cells in the lumen indicates that functional capillary networks were formed between the host vasculature and the human-specific luminal structures created by the implanted cells. Injection of the Matrigel alone resulted in no vascular network formation (data not shown). The specificity of the human CD31 antibody and UEA-1 lectin was confirmed by negative staining of mouse aorta (data not shown).

DISCUSSION

Tissue neovascularization may in itself treat diseases such as myocardial and peripherovascular ischemia, and it is increasingly recognized as an essential ingredient for the successful engineering and transplantation of bone, liver and a range of other tissues (11,27,28,32,36,44,47). Neovascularization will not occur in the absence of EC.

Classical sources of human EC have been umbilical vein (HUVEC) and MVEC from foreskin (8,15,16). However, in a therapeutic setting these cells will almost always be allogeneic to the patient. A new paradigm was established with the identification of EPC (2). Human EPC can be isolated from the blood and expanded to clinically relevant numbers, but this requires extended in vitro culture (24,34). Recently, MSC have been identified as important for neovascularization because they seem to have a role as pericytes in most tissues (7). Thus, the establishment of robust tissue vascularization may require at least two cell types: EC and MSC/pericytes. We have previously purified and characterized MSC from AT, and have shown how they can be obtained as primary uncultured cells in large numbers (4). The present study identifies AT as a source also of EC. AT-EC, too, can be obtained in large numbers as primary uncultured cells, and they, too, are readily expanded in vitro. The negative selection strategy allows the isolation of AT-EC with high purity, and with no contamination in the cell culture of the immunobeads used for selection. As AT is easily obtainable from all patients, an autologous source of the most important cells required for vasculogenesis should now be readily available in most therapeutic situations.

It is a little difficult to place the AT-EC within the established EC hierarchy. As they do not express either isoform of CD133, and do express CD144 (VE-cadherin) and vWF, they are not early EPC (13,43). At the other end of the hierarchy, human MVEC have been shown to strongly express CD141 (3), which was only weakly or not expressed on the cells characterized here. AT-EC most resemble late EPC based on the phenotype $CD34^+CD133^-vWF^+CD144^+VEGFR-2^+eNOS^+CD31^+$ (13,43). However, if almost unlimited in vitro expansion potential is required for cells to deserve the “progenitor” designation, then the AT-EC are not EPC. This was shown by Melero-Martin et al. to be

a property of human blood-derived endothelial progenitor cells (24). In contrast, our AT-EC ceased to proliferate after 14 – 19 passages. Consequently, these cells are most likely differentiated EC with high in vitro proliferative capacity.

Although we were able to isolate high numbers of primary AT-EC, in vitro expansion was necessary to obtain the number of cells that will likely be needed in most protocols of in vivo vasculogenesis (21,25,29,35,48). For instance, 10^8 cells could be obtained after only a few passages. At this time the cells were in a log phase of growth and showed the classical cobblestone morphology, but certain changes had already been induced by in vitro culture. On the cell surface, CD34, CD90 and HLA DR had quickly disappeared. Interestingly, *CD34* and *THY1* (CD90) mRNA were maintained for some time after the cell surface expression was lost, suggesting that these phenotypes might possibly be induced under other culture conditions. For comparison, CD90 and HLA-DR were also found not to be expressed on blood-derived human EPC, while CD34 was reported to be expressed on these cultured cells (24,34). Equally strikingly, CD44 changed from being practically absent on the uncultured AT-EC, which were depleted for CD44 expressing cells, to being gradually more expressed. The depletion procedure was sufficiently efficient to strongly suggest that this was a bona fide change in phenotype, and not an outgrowth of a small subset with an otherwise similar phenotype. At p12, a very large proportion of the cells expressed CD44. A similar, although less dramatic change was noted for VEGFR-2 and vWF. For both these markers a parallel increase was noted at the mRNA level.

The functional properties of the AT-EC were examined using vasculogenesis assays. In vitro, the AT-EC formed tubes similar to the commercially obtained MVEC used for positive control. Interestingly, we also observed very efficient tube formation using

cells obtained from late passages suggesting that the AT-EC retain their functional capacity better than cord blood-derived EPC, which were found to lose functional capacity upon in vitro passaging (24). To our surprise, uncultured AT-EC did not form tubes in Matrigel in vitro. To the best of our knowledge, this assay has not been performed on any population of uncultured EC before, presumably because the different primary EC populations described to date have been too few to perform assays of this nature. While it is likely that the AT-EC, given the right stimulus, would be able to create new vessels in vivo, the in vitro vasculogenesis assay presented here may be able to elicit vasculogenic properties only from the in vitro cultured EC to which it has been adapted. Results from the in vivo blood vessel forming assay showed that AT-EC alone were able to form vessels containing mouse-derived erythrocytes. However, these results were inconsistent, and in all cases the vessel formation was denser and more consistent when AT-MSCs were added to the Matrigel. More experiments must be performed, perhaps also using in vivo ischemia models of neovascularization, in order to support these observations with statistics. It makes sense, though, to think that addition of pericytes to EC will yield more robust blood vessels. After all, these cultured cells probably derive from the very cells that made up the layers of the walls of the small vessels in the AT from which they were isolated (6,42). Hopefully this combination of autologous cells may, in the future, be shown to provide blood supply to ischemic tissues in vivo or a vascular network for in vitro engineered tissue implants.

ACKNOWLEDGEMENTS

The authors thank Colosseum Klinikken, Oslo (Tone Irene Langslet) for kindly providing liposuction material, Linda T. Dorg and Finn P. Reinholt for sectioning and H&E staining, Peter Hofgaard and Bjarne Bogen for help with the animal experiments, Axel M. K uchler for helpful suggestions pertaining to immunohistochemistry, Steven Hoel for advice, support and discussions.

This work was supported by a Storforsk grant from the Norwegian Research Council.

DISCLOSURE STATEMENT

The authors declare no competing financial interest.



REFERENCES

1. Arts, C. H.; de Groot, P.; Heijnen-Snyder, G. J.; Blankensteijn, J. D.; Eikelboom, B. C.; Slaper-Cortenbach, I. C. Application of a clinical grade CD34-mediated method for the enrichment of microvascular endothelial cells from fat tissue. *Cytotherapy* 6:30-42; 2004.
2. Asahara, T.; Murohara, T.; Sullivan, A.; Silver, M.; van der Zee, R.; Li, T.; Witzendichler, B.; Schatteman, G.; Isner, J. M. Isolation of putative progenitor endothelial cells for angiogenesis. *Science* 275:964-967; 1997.
3. Bagley, R. G.; Walter-Yohrling, J.; Cao, X.; Weber, W.; Simons, B.; Cook, B. P.; Chartrand, S. D.; Wang, C.; Madden, S. L.; Teicher, B. A. Endothelial precursor cells as a model of tumor endothelium: characterization and comparison with mature endothelial cells. *Cancer Res.* 63:5866-5873; 2003.
4. Boquest, A. C.; Shahdadfar, A.; Fronsdal, K.; Sigurjonsson, O.; Tunheim, S. H.; Collas, P.; Brinchmann, J. E. Isolation and transcription profiling of purified uncultured human stromal stem cells: alteration of gene expression after in vitro cell culture. *Mol. Biol. Cell* 16:1131-1141; 2005.
5. Covas, D. T.; Panepucci, R. A.; Fontes, A. M.; Silva, W. A., Jr.; Orellana, M. D.; Freitas, M. C.; Neder, L.; Santos, A. R.; Peres, L. C.; Jamur, M. C.; Zago, M. A. Multipotent mesenchymal stromal cells obtained from diverse human tissues share

functional properties and gene-expression profile with CD146+ perivascular cells and fibroblasts. *Exp. Hematol.* 36:642-654; 2008.

6. Crisan, M.; Yap, S.; Casteilla, L.; Chen, C. W.; Corselli, M.; Park, T. S.; Andriolo, G.; Sun, B.; Zheng, B.; Zhang, L.; Norotte, C.; Teng, P. N.; Traas, J.; Schugar, R.; Deasy, B. M.; Badylak, S.; Buhring, H. J.; Giacobino, J. P.; Lazzari, L.; Huard, J.; Peault, B. A perivascular origin for mesenchymal stem cells in multiple human organs. *Cell Stem Cell* 3:301-313; 2008.

7. da Silva, M. L.; Caplan, A. I.; Nardi, N. B. In search of the in vivo identity of mesenchymal stem cells. *Stem Cells* 26:2287-2299; 2008.

8. Davison, P. M.; Bensch, K.; Karasek, M. A. Isolation and growth of endothelial cells from the microvessels of the newborn human foreskin in cell culture. *J. Invest. Dermatol.* 75:316-321; 1980.

9. Herrmann, J. L.; Abarbanell, A. M.; Weil, B. R.; Wang, Y.; Wang, M.; Tan, J.; Meldrum, D. R. Cell-based therapy for ischemic heart disease: a clinical update. *Ann. Thorac. Surg.* 88:1714-1722; 2009.

10. Hewett, P. W. Vascular endothelial cells from human micro- and macrovessels: isolation, characterisation and culture. *Methods Mol. Biol.* 467:95-111; 2009.

11. Hoganson, D. M.; Pryor, H. I.; Vacanti, J. P. Tissue engineering and organ structure: a vascularized approach to liver and lung. *Pediatr. Res.* 63:520-526; 2008.
12. Hong, S. J.; Traktuev, D. O.; March, K. L. Therapeutic potential of adipose-derived stem cells in vascular growth and tissue repair. *Curr. Opin. Organ Transplant.* 15:86-91; 2010.
13. Hristov, M.; Weber, C. Endothelial progenitor cells: characterization, pathophysiology, and possible clinical relevance. *J. Cell. Mol. Med.* 8:498-508; 2004.
14. Hung, H. S.; Shyu, W. C.; Tsai, C. H.; Hsu, S. H.; Lin, S. Z. Transplantation of endothelial progenitor cells as therapeutics for cardiovascular diseases. *Cell Transplant.* 18:1003-1012; 2009.
15. Jackson, C. J.; Garbett, P. K.; Nissen, B.; Schrieber, L. Binding of human endothelium to *Ulex europaeus* I-coated Dynabeads: application to the isolation of microvascular endothelium. *J. Cell Sci.* 96(Pt 2):257-262; 1990.
16. Jaffe, E. A.; Nachman, R. L.; Becker, C. G.; Minick, C. R. Culture of human endothelial cells derived from umbilical veins. Identification by morphologic and immunologic criteria. *J. Clin. Invest.* 52:2745-2756; 1973.

17. Kent, K. C.; Shindo, S.; Ikemoto, T.; Whittemore, A. D. Species variation and the success of endothelial cell seeding. *J. Vasc. Surg.* 9:271-276; 1989.
18. Kern, P. A.; Knedler, A.; Eckel, R. H. Isolation and culture of microvascular endothelium from human adipose tissue. *J. Clin. Invest.* 71:1822-1829; 1983.
19. Koyama, M.; Satoh, K.; Yoshida, H.; Suzuki, S.; Koie, H.; Takamatsu, S. Surface coverage of vascular grafts with cultured human endothelial cells from subcutaneous fat tissue obtained with a biopsy needle. *Thromb. Haemost.* 76:610-614; 1996.
20. Lee, E. J.; Vunjak-Novakovic, G.; Wang, Y.; Niklason, L. E. A biocompatible endothelial cell delivery system for in vitro tissue engineering. *Cell Transplant.* 18:731-743; 2009.
21. Li, Z.; Han, Z.; Wu, J. C. Transplantation of human embryonic stem cell-derived endothelial cells for vascular diseases. *J. Cell. Biochem.* 106:194-199; 2009.
22. Livak, K. J.; Schmittgen, T. D. Analysis of relative gene expression data using real-time quantitative PCR and the $2^{-\Delta\Delta C(T)}$ Method. *Methods* 25:402-408; 2001.
23. Mandarino, L. J.; Sundarraj, N.; Finlayson, J.; Hassell, H. R. Regulation of fibronectin and laminin synthesis by retinal capillary endothelial cells and pericytes in vitro. *Exp. Eye Res.* 57:609-621; 1993.

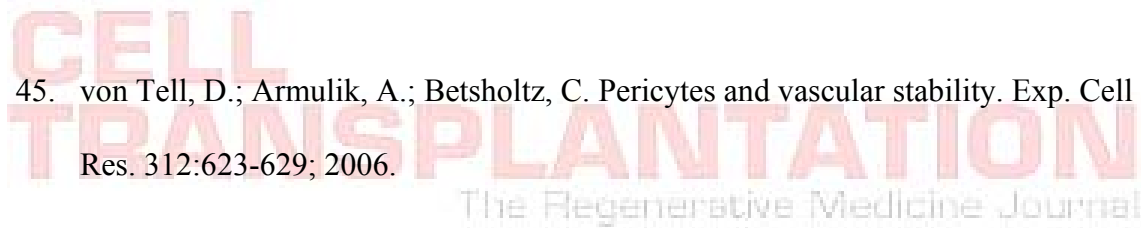
24. Melero-Martin, J. M.; Khan, Z. A.; Picard, A.; Wu, X.; Paruchuri, S.; Bischoff, J. In vivo vasculogenic potential of human blood-derived endothelial progenitor cells. *Blood* 109:4761-4768; 2007.
25. Menasche, P.; Hagege, A. A.; Vilquin, J. T.; Desnos, M.; Abergel, E.; Pouzet, B.; Bel, A.; Sarateanu, S.; Scorsin, M.; Schwartz, K.; Bruneval, P.; Benbunan, M.; Marolleau, J. P.; Duboc, D. Autologous skeletal myoblast transplantation for severe postinfarction left ventricular dysfunction. *J. Am. Coll. Cardiol.* 41:1078-1083; 2003.
26. Miranville, A.; Heeschen, C.; Sengenès, C.; Curat, C. A.; Busse, R.; Bouloumie, A. Improvement of postnatal neovascularization by human adipose tissue-derived stem cells. *Circulation* 110:349-355; 2004.
27. Nomi, M.; Atala, A.; Coppi, P. D.; Soker, S. Principals of neovascularization for tissue engineering. *Mol. Aspects Med.* 23:463-483; 2002.
28. Pepper, M. S. Manipulating angiogenesis. From basic science to the bedside. *Arterioscler. Thromb. Vasc. Biol.* 17:605-619; 1997.
29. Perin, E. C.; Silva, G. V. Autologous cell-based therapy for ischemic heart disease: clinical evidence, proposed mechanisms of action, and current limitations. *Catheter Cardiovasc. Interv.* 73:281-288; 2009.

30. Planat-Benard, V.; Silvestre, J. S.; Cousin, B.; Andre, M.; Nibbelink, M.; Tamarat, R.; Clergue, M.; Manneville, C.; Saillan-Barreau, C.; Duriez, M.; Tedgui, A.; Levy, B.; Penicaud, L.; Casteilla, L. Plasticity of human adipose lineage cells toward endothelial cells: physiological and therapeutic perspectives. *Circulation* 109:656-663; 2004.
31. Prater, D. N.; Case, J.; Ingram, D. A.; Yoder, M. C. Working hypothesis to redefine endothelial progenitor cells. *Leukemia* 21:1141-1149; 2007.
32. Rafii, S.; Lyden, D. Therapeutic stem and progenitor cell transplantation for organ vascularization and regeneration. *Nat. Med.* 9:702-712; 2003.
33. Rehman, J.; Traktuev, D.; Li, J.; Merfeld-Clauss, S.; Temm-Grove, C. J.; Bovenkerk, J. E.; Pell, C. L.; Johnstone, B. H.; Considine, R. V.; March, K. L. Secretion of angiogenic and antiapoptotic factors by human adipose stromal cells. *Circulation* 109:1292-1298; 2004.
34. Reinisch, A.; Hofmann, N. A.; Obenauf, A. C.; Kashofer, K.; Rohde, E.; Schallmoser, K.; Flicker, K.; Lanzer, G.; Linkesch, W.; Speicher, M. R.; Strunk, D. Humanized large-scale expanded endothelial colony-forming cells function in vitro and in vivo. *Blood* 113:6716-6725; 2009.
35. Rosenzweig, A. Cardiac cell therapy--mixed results from mixed cells. *N. Engl. J. Med.* 355:1274-1277; 2006.

36. Seebach, C.; Henrich, D.; Kaehling, C.; Wilhelm, K.; Tami, A.; Alini, M.; Marzi, I. Endothelial progenitor cells and mesenchymal stem cells seeded onto beta-TCP granules enhance early vascularization and bone healing in a critical size bone defect in rats. *Tissue Eng. Part A* 16:1961-1970; 2010.
37. Sharp, W. V.; Schmidt, S. P.; Meerbaum, S. O.; Pippert, T. R. Derivation of human microvascular endothelial cells for prosthetic vascular graft seeding. *Ann. Vasc. Surg.* 3:104-107; 1989.
38. Shepro, D.; Morel, N. M. Pericyte physiology. *FASEB J.* 7:1031-1038; 1993.
39. Shieh, S. J.; Vacanti, J. P. State-of-the-art tissue engineering: from tissue engineering to organ building. *Surgery* 137:1-7; 2005.
40. Tateishi-Yuyama, E.; Matsubara, H.; Murohara, T.; Ikeda, U.; Shintani, S.; Masaki, H.; Amano, K.; Kishimoto, Y.; Yoshimoto, K.; Akashi, H.; Shimada, K.; Iwasaka, T.; Imaizumi, T. Therapeutic angiogenesis for patients with limb ischaemia by autologous transplantation of bone-marrow cells: a pilot study and a randomised controlled trial. *Lancet* 360:427-435; 2002.
41. Tilton, R. G. Capillary pericytes: perspectives and future trends. *J. Electron Microsc. Tech.* 19:327-344; 1991.
42. Traktuev, D. O.; Merfeld-Clauss, S.; Li, J.; Kolonin, M.; Arap, W.; Pasqualini, R.; Johnstone, B. H.; March, K. L. A population of multipotent CD34-positive

adipose stromal cells share pericyte and mesenchymal surface markers, reside in a periendothelial location, and stabilize endothelial networks. *Circ. Res.* 102:77-85; 2008.

43. Urbich, C.; Dimmeler, S. Endothelial progenitor cells functional characterization. *Trends Cardiovasc. Med.* 14:318-322; 2004.
44. Verseijden, F.; Posthumus-van Sluijs, S. J.; Farrell, E.; van Neck, J. W.; Hovius, S. E.; Hofer, S. O.; van Osch, G. J. Prevascular structures promote vascularization in engineered human adipose tissue constructs upon implantation. *Cell Transplant.* 19:1007-1020; 2010.
45. von Tell, D.; Armulik, A.; Betsholtz, C. Pericytes and vascular stability. *Exp. Cell Res.* 312:623-629; 2006.
46. Wester, T.; Jorgensen, J. J.; Stranden, E.; Sandbaek, G.; Tjonnfjord, G.; Bay, D.; Kollerros, D.; Kroese, A. J.; Brinchmann, J. E. Treatment with autologous bone marrow mononuclear cells in patients with critical lower limb ischaemia. A pilot study. *Scand. J. Surg.* 97:56-62; 2008.
47. Yu, H.; VandeVord, P. J.; Mao, L.; Matthew, H. W.; Wooley, P. H.; Yang, S. Y. Improved tissue-engineered bone regeneration by endothelial cell mediated vascularization. *Biomaterials* 30:508-517; 2009.



48. Zampetaki, A.; Kirton, J. P.; Xu, Q. Vascular repair by endothelial progenitor cells. *Cardiovasc. Res.* 78:413-421; 2008.
49. Zuk, P. A.; Zhu, M.; Ashjian, P.; De Ugarte, D. A.; Huang, J. I.; Mizuno, H.; Alfonso, Z. C.; Fraser, J. K.; Benhaim, P.; Hedrick, M. H. Human adipose tissue is a source of multipotent stem cells. *Mol. Biol. Cell* 13:4279-4295; 2002.
50. Zuk, P. A.; Zhu, M.; Mizuno, H.; Huang, J.; Futrell, J. W.; Katz, A. J.; Benhaim, P.; Lorenz, H. P.; Hedrick, M. H. Multilineage cells from human adipose tissue: implications for cell-based therapies. *Tissue Eng.* 7:211-228; 2001.



Table 1: List of primers used in real-time RT-PCR

Gene title	Gene symbol	TaqMan assay number (Applied Biosystems)
von Willebrand factor (vWF)	<i>VWF</i>	Hs00169795_m1
Endothelial nitric oxide synthase (eNOS)	<i>NOS3</i>	Hs00167166_m1
Vascular endothelial cadherin (VE-cadherin)	<i>CDH5</i>	Hs00174344_m1
Platelet endothelial cell adhesion molecule-1 (CD31)	<i>PECAM1</i>	Hs00169777_m1
Vascular endothelial growth factor receptor 2 (VEGFR2)	<i>KDR</i>	Hs00176676_m1
CD44	<i>CD44</i>	Hs01075861_m1
CD90	<i>THY1</i>	Hs00174816_m1
CD34	<i>CD34</i>	Hs00156373_m1
Cyclin-dependent kinase inhibitor 1A	<i>CDKN1A</i>	Hs00355782_m1

The Regenerative Medicine Journal

Table 2: List of antibodies used in flow cytometry

Fluorescein isothiocyanate (FITC) conjugated antibodies	Clone	Company
CD3	UCHT-1	Diatec Monoclonal AS, Oslo, Norway
CD31 (PECAM-1)	WM-59	AbD Serotec, Oxford, UK
CD34	581	BD Biosciences, San Jose, CA
CD44	F10-44-2	Southern Biotech, Birmingham, AL
CD102 (ICAM-2)	B-T1	AbD Serotec, Oxford, UK
CD106 (VCAM-1)	1GIIB1	AbD Serotec, Oxford, UK
CD141 (Thrombomodulin)	B-A35	Chemicon International, Millipore, Billerica, MA
CD146 (P1H12)	OJ 79c	AbD Serotec, Oxford, UK
HLA-DR	L243	BD Biosciences, San Jose, CA
UEA-1	-----	Sigma Aldrich, St. Louis, MO

Phycoerythrin (PE) conjugated antibodies	Clone	Company
CD14	18D11	Diatec Monoclonal AS, Oslo, Norway
CD45	E01	Diatec Monoclonal AS, Oslo, Norway
CD62E (E-selectin)	P2H3	eBioscience, San Diego, CA
CD90 (Thy-1)	5E10	BD Biosciences, San Jose, CA
CD144 (VE-cadherin)	16B1	eBioscience, San Diego, CA
VEGFR-1 (Flt-1)	49560	R&D Systems, Abingdon, Oxon, UK
VEGFR-2 (Flk-1)	89106	R&D Systems, Abingdon, Oxon, UK
vWF	4F9	Immunotech, Marseille, France

Allophycocyanin (APC) conjugated antibodies	Clone	Company
CD19	AE1	Diatec Monoclonal AS, Oslo, Norway
CD31 (PECAM-1)	WM-59	eBioscience, San Diego, CA
CD105 (endoglin)	SH2	Diatec Monoclonal AS, Oslo, Norway
CD133-1	AC133	Miltenyi Biotec, Bergisch Gladbach, Germany
CD133-2	293C3	Miltenyi Biotec, Bergisch Gladbach, Germany
CD202b (Tie-2)	83715	R&D Systems, Abingdon, Oxon, UK

Cy-Chrome (CY) conjugated antibodies	Clone	Company
CD54 (ICAM-1)	HA58	BD Biosciences, San Jose, CA
HLA-ABC	G46-2.6	BD Biosciences, San Jose, CA

ICAM = Intercellular adhesion molecule; VCAM = vascular cell adhesion molecule; HLA = human lymphocyte antigen; UEA-1 = Ulex europaeus agglutinin 1

Figure legends

Figure 1. Growth kinetics and phase contrast morphology of adipose tissue derived endothelial cells (AT-EC). (A) Light microscopy of a confluent monolayer of AT-EC (passage 8) exhibiting typical cobblestone morphology. Cultures were examined by a Leica DMIL inverted microscope. Image was taken with a Leica DFC 320 camera using Adobe Photoshop 7.0 software and a 10x/0.22 Leica objective lens. Scale bar represents 100µm. (B) Calculated accumulated cell counts from cultures of AT-EC isolated from three different donors.

Figure 2. Real-time reverse transcription-polymerase chain reaction (RT-PCR) analysis. Graphs represents expression of mRNA encoding endothelial markers *CD31/PECAM1*; *CD34*; *VEGFR-2/KDR*; *VWF*; *NOS3*; VE-cadherin/*CDH5*, and mesenchymal stem cell (MSC) markers *CD90/THY1*; *CD44* at different passages (p0 = uncultured cells; p2 = passage 2; p6 = passage 6; p12 = passage 12) in three donors. Graphs were created using GraphPad Prism 5 software.

Figure 3. Gene expression, in vitro vasculogenic potential and cell surface marker expression of primary adult human dermal microvascular endothelial cells (MVEC). (A) Real-time RT-PCR analysis. Graphs represents expression of mRNA encoding endothelial markers *CD31/PECAM1*; *CD34*; *VEGFR-2/KDR*; *VWF*; *NOS3*; VE-cadherin/*CDH5*, and MSC markers *CD90/THY1*; and *CD44* at passage 6. Graphs were created using GraphPad Prism 5 software. (B) In vitro vasculogenesis assay. MVEC (p6) create extensive capillary-like structures in Matrigel. Vascular network was

examined after 20 hours by a Leica DMIL inverted microscope. Image was taken with a Leica DFC 320 camera using Adobe Photoshop 7.0 software and a 10x/0.22 Leica objective lens. Scale bar represents 100 μ m. (C) Flow cytometric analysis. Flow cytometry histograms of cells from passage 6. Gray histograms represent cells stained with fluorescent antibodies conjugated to fluorescein isothiocyanate (FITC), allophycocyanin (APC), phycoerythrin (PE) and phycoerythrin-cyanin 5 (PE-Cy5). Isotype-matched control antibodies are overlaid in a black line on each histogram.

Figure 4. Flow cytometric analysis. (A) Cell surface marker expression of the stromal vascular fraction (SVF). (B) Purity and phenotype change of AT-EC at different passages. Flow cytometry plots of cells from donor 3 (A) and donor 2 (B), representative of the three donors. Cells were co-stained for CD31 (platelet endothelial cell adhesion molecule, PECAM), CD90 (Thy-1), CD44 (homing-associated cell adhesion molecule, H-CAM) and CD45. Isotype matched control fluorescent antibodies were used as negative controls.

Figure 5. Flow cytometric characterization of AT-EC. Flow cytometry histograms of cells from donor 3, representative of the three donors at different passages. Gray histograms represent cells stained with fluorescent antibodies conjugated to (A) fluorescein isothiocyanate (FITC), (B) allophycocyanin (APC), (C) phycoerythrin (PE) and (D) phycoerythrin-cyanin 5 (PE-Cy5). Isotype-matched control antibodies are overlaid in a black line on each histogram.

Figure 6. DiI complex acetylated low-density lipoprotein (DiI-Ac-LDL) uptake. (A) Uptake of DiI-Ac-LDL by AT-EC, and (B) by human chondrocytes and (C) adipose tissue derived mesenchymal stem cells (AT-MSC) used as negative controls. Scale bars represent 50 μ m (A) and 100 μ m (B, C). 4',6-diamidino-2-phenylindole (DAPI) stains the nuclei in blue in each image. Slides were assessed using a Nikon, Eclipse E600 fluorescent microscope equipped with Nikon 20x/0.45 and 40x/0.75 objective lenses and Leica DC 300F and Color View III digital cameras. Images were taken using Adobe Photoshop 7.0 and Cell B software.

Figure 7. In vitro vasculogenesis assay. Representative images of vascular network formation on Matrigel. (A) Freshly isolated AT-EC are not able to form vascular tubes while seeded on Matrigel. (B) Cultured AT-EC (p2) create extensive capillary-like structures in Matrigel. (C) Image showing tube formation ability of AT-EC (p2) following PKH67 fluorescent cell labeling of AT-EC. (D) Extensive capillary-like network formed by late passage AT-EC (p13). (E) AT-MSC and (F) AT-MSC mixed with AT-EC were not able to form capillary-like networks in Matrigel. Vascular network was examined after 20 hours by a Leica DMIL inverted microscope. Images were taken with a Leica DFC 320 camera using Adobe Photoshop 7.0 software and 4x/0.10 and 10x/0.22 Leica objective lenses. Scale bars represent 50 μ m (B) and 100 μ m (A, C, D, E, F).

Figure 8. In vivo vasculogenic potential of AT-EC. (A, D) Representative fluorescence images of human specific CD31 (Cy3) and (B, E) human specific *Ulex europaeus* agglutinin I lectin (UEA-1) (FITC) staining at 400x and 1000x magnification. (C, F)

Merged images of CD31 and UEA-1 staining. Scale bars represent 50 and 10 μ m, respectively. DAPI stains the nuclei in blue in each image. White arrows indicate the position of the vascular lumen and the endothelium. Mouse red blood cells within the vascular lumen are seen to emit both red and green autofluorescence. Slides were assessed using a Nikon Eclipse E600 fluorescent microscope equipped with Nikon 40x0.75 and 100x/1.30 Oil objective lenses and a Leica DC 300F digital camera. Images were taken using Adobe Photoshop 7.0 software. All images were assembled into multipanel figures using Adobe Illustrator CS4 (Adobe Systems Norge AS, Oslo, Norway).

CELL TRANSPLANTATION

The Regenerative Medicine Journal

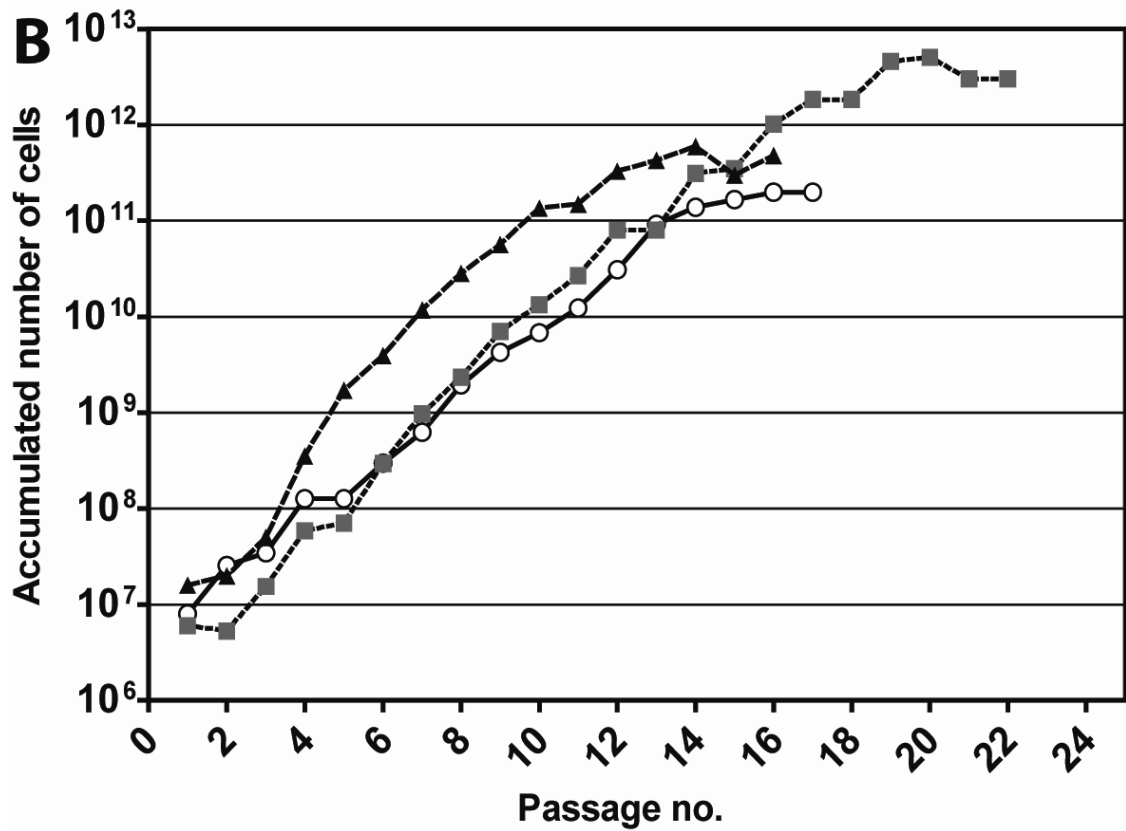
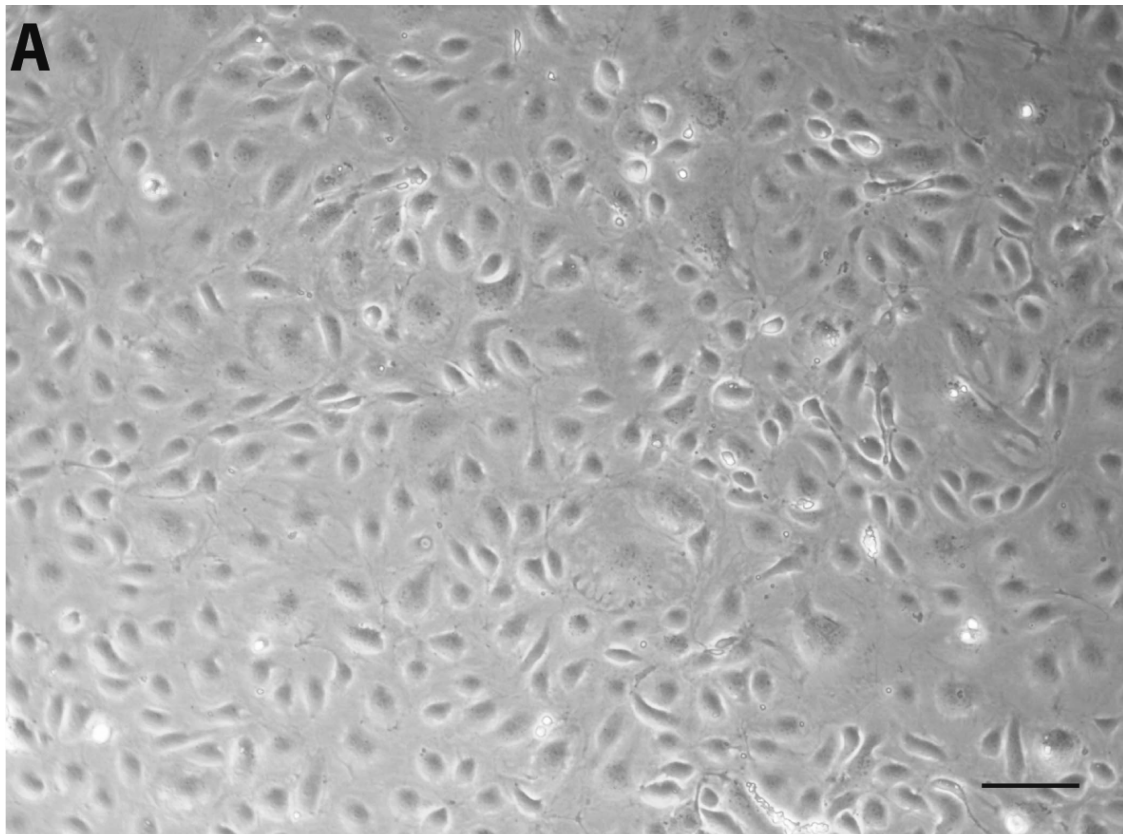


Figure 1:

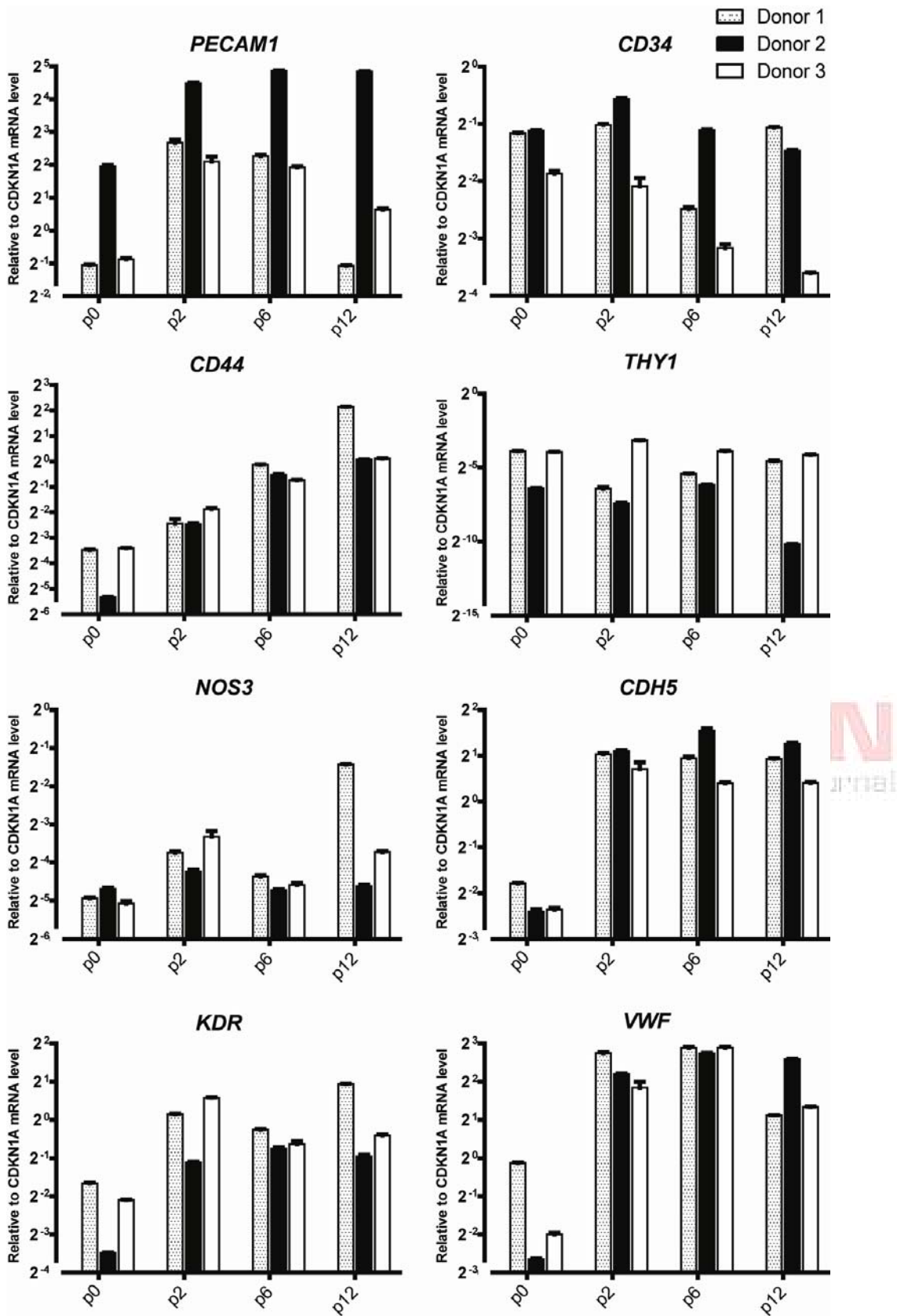
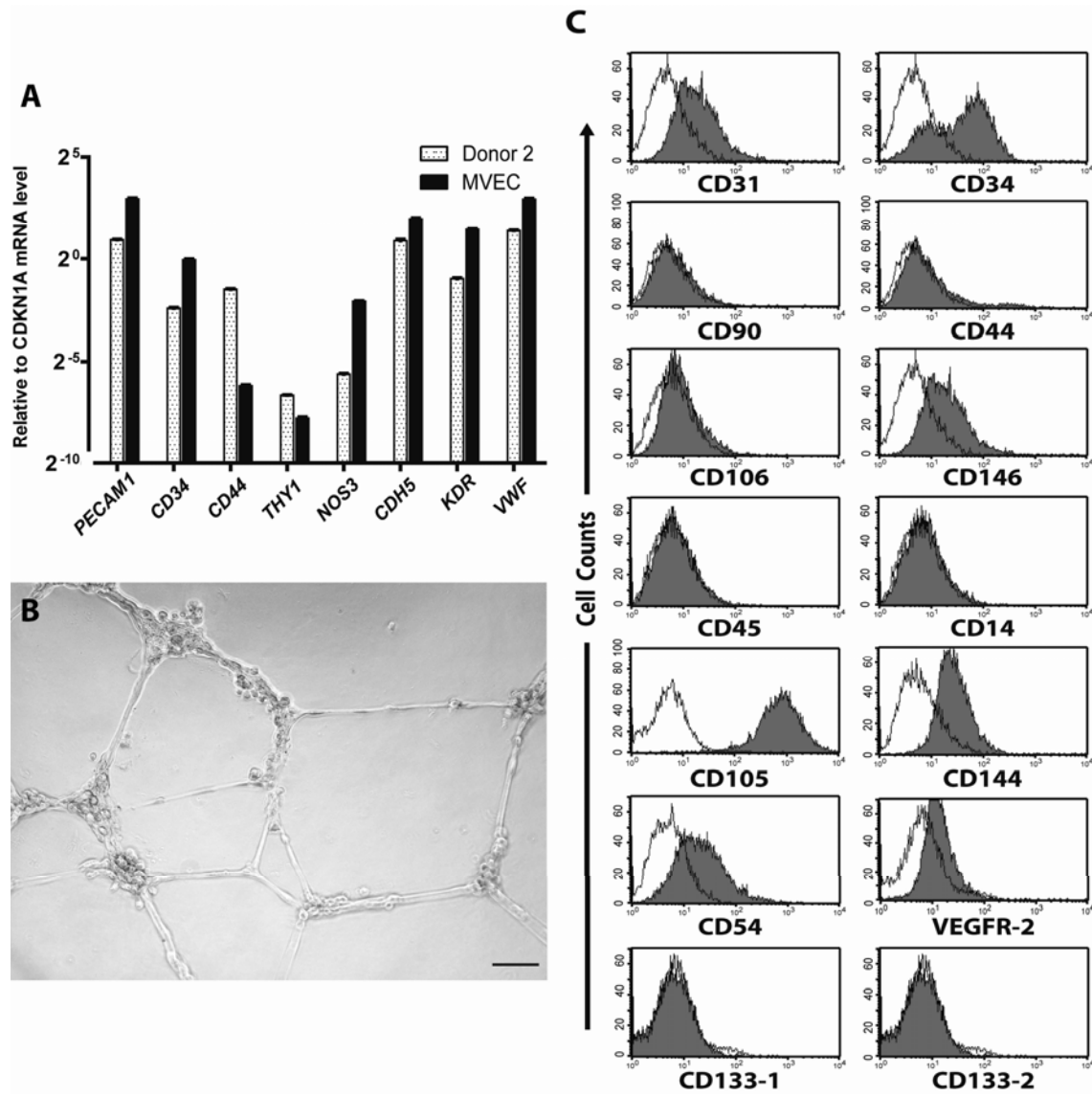


Figure 2:



ATION
Medicine Journal

Figure 3:

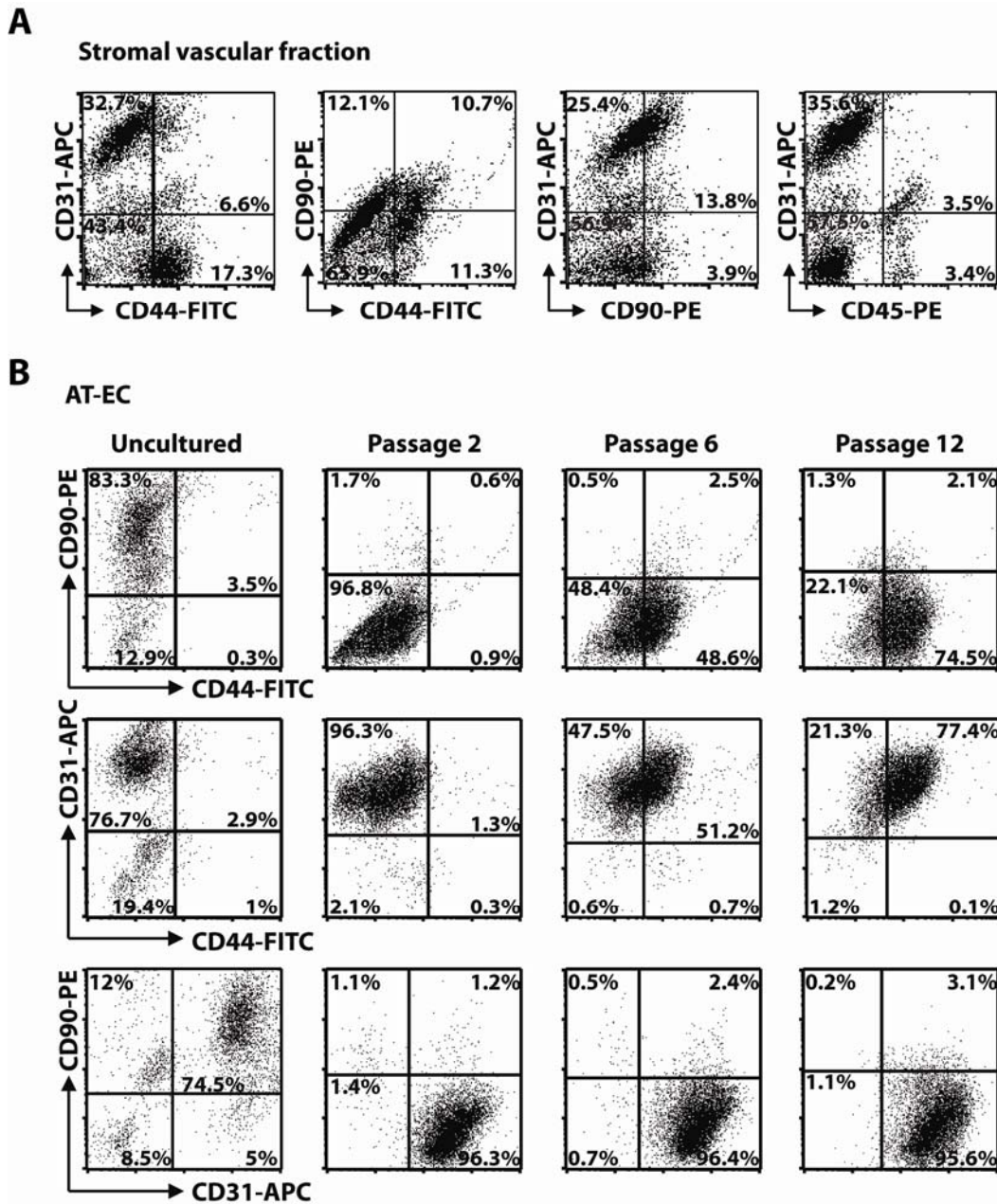
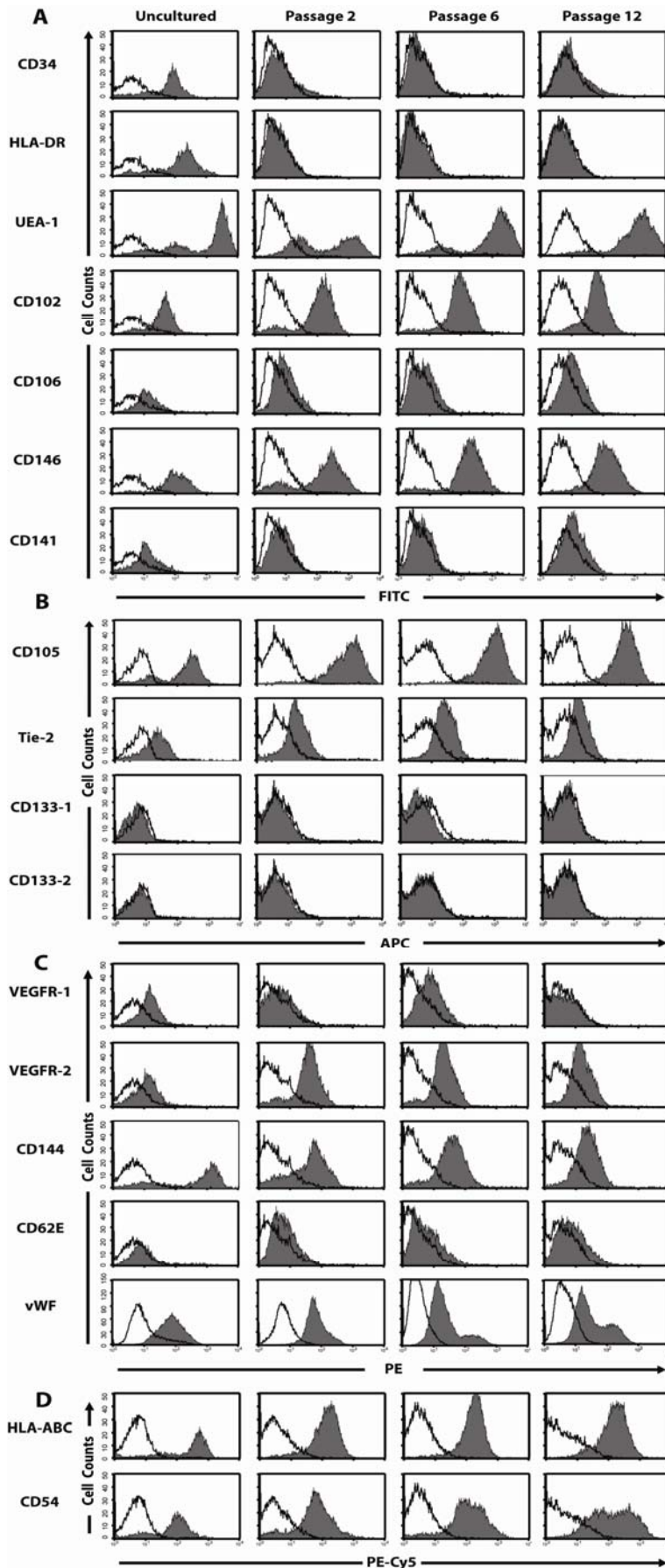


Figure 4:



ATION
Medicine Journal

Figure 5:



ATION
e Medicine Journal

Figure 6:

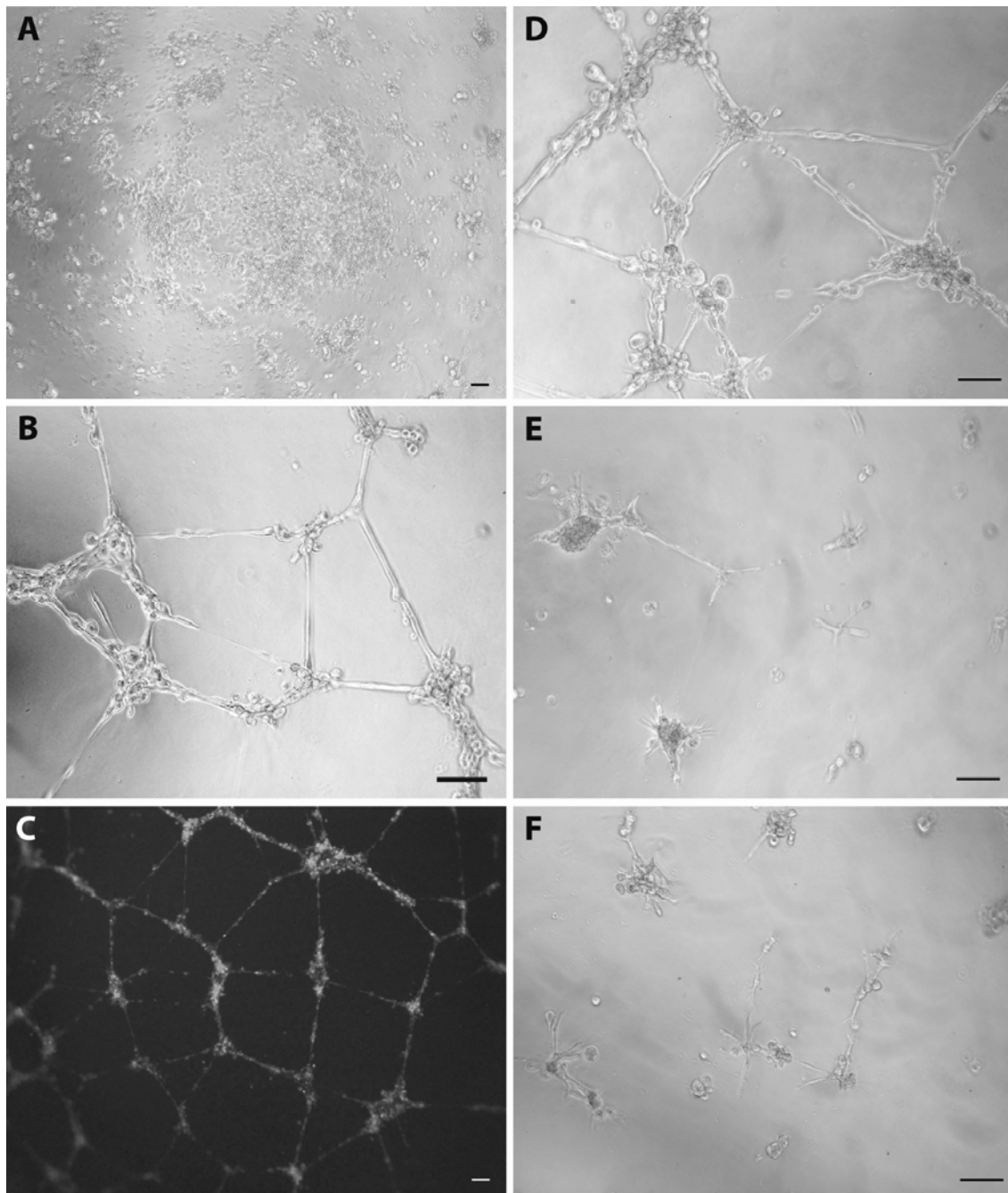


Figure 7:

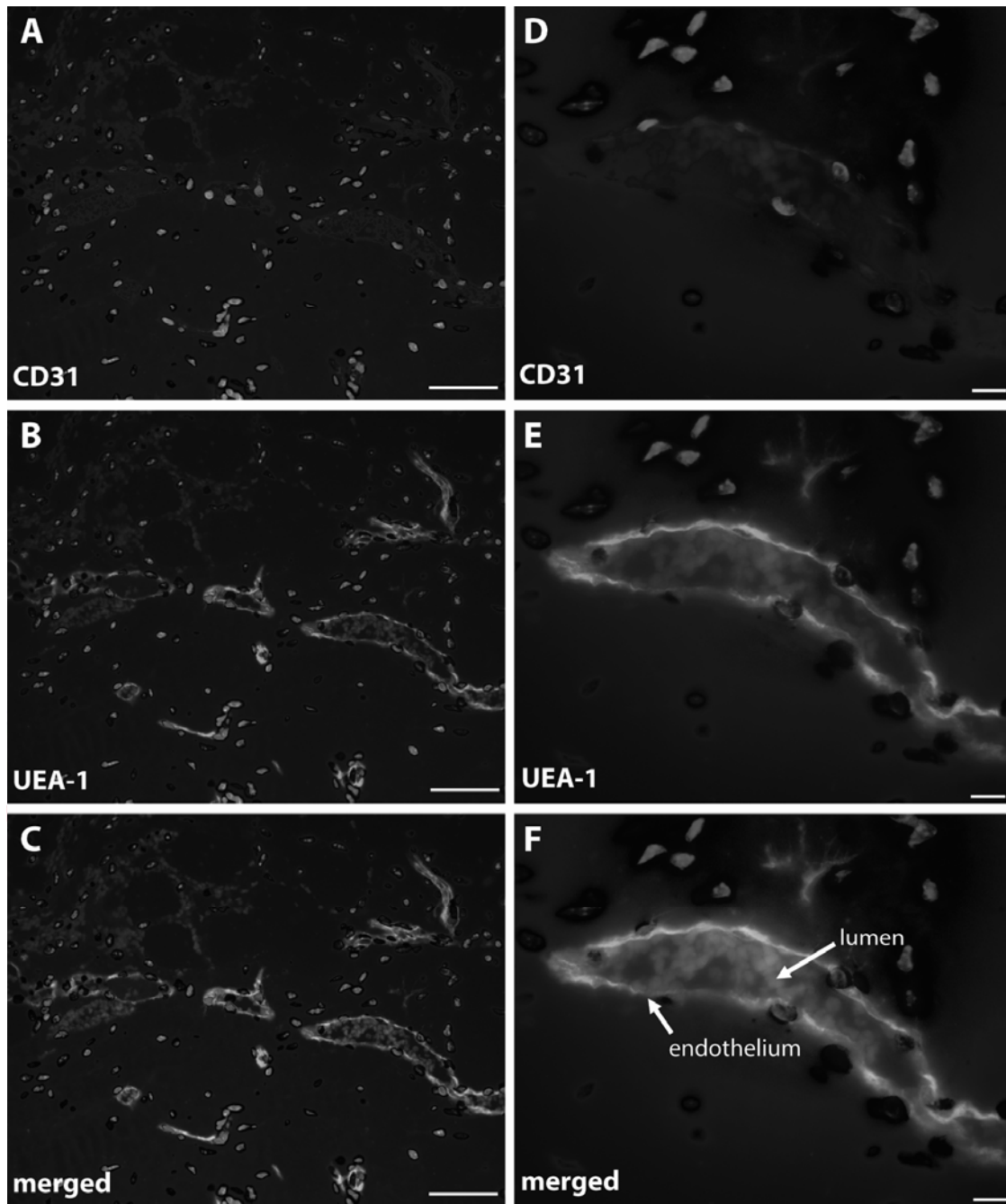


Figure 8: